Defect modes in helical photonic crystals: An analytic approach

M. Becchi, S. Ponti, J. A. Reyes,* and C. Oldano
Dipartimento di Fisica Politecnico di Torino and INFM Corso Duca degli Abruzzi 24, 10129 Torino, Italy
(Received 8 May 2003; revised manuscript received 9 April 2004; published 16 July 2004)

Considering helically periodic structures with a twist defect, we define the defect mode in unbounded media and the scattering properties of bounded samples. The mode frequency, the lifetime of the defect mode, and the spectral width of the transmittance and reflectance peaks are expressed by fully analytic and very simple equations, the simplest ones appearing in the literature of photonic band gap materials. Our approach provides a clear explanation of the interesting optical properties of lossless samples with a twist defect and shows that the absorption greatly changes such properties, giving rise to unexpected effects. In particular, the total absorption within thick samples can decrease drastically when the absorption coefficient is increased beyond a well defined value.

DOI: 10.1103/PhysRevB.70.033103 PACS number(s): 42.70.Qs, 42.70.Df

Cholesteric liquid crystals have been the object of intense research during the last century for their interesting optical properties and because they are the unique periodic structures admitting analytic solutions of Maxwell equations based on very simple algebraic expressions.[1] Recently it has been possible to insert defects in cholestericlike structures, thus obtaining a type of photonic band gap materials,[2] which are of increasing interest for applications in linear and nonlinear optics.[2–7] In this paper, we develop a general theory for helical samples with twist defects, which extends to these structures the modal analysis given in Ref. 1 for perfectly periodic cholesterics.

At the two sides of the defect plane the electromagnetic field can be written as a superposition of the four eigenwaves $1^{\pm}$ and $2^{\pm}$ of the periodic structure without defects. We consider here axial propagation of monochromatic light in a locally uniaxial medium, optically defined by the permittivity and permeability tensors $\epsilon_o\epsilon$ and $\mu_o\mu$, whose optical axis is everywhere orthogonal to the axis x_3 and rotates uniformly along x_3. The well-known propagation equation can be written as $d\alpha/dx_3 = i(\omega/c)H\alpha$, where

$$\alpha = \begin{pmatrix} e_1 \\ e_2 \\ h_1 \\ h_2 \end{pmatrix}; \quad H = \begin{pmatrix} 0 & -i\tilde{q} & 0 & \mu_2 \\ i\tilde{q} & 0 & -\mu_1 & 0 \\ 0 & -\epsilon_2 & 0 & -i\tilde{q} \\ \epsilon_1 & 0 & i\tilde{q} & 0 \end{pmatrix}, \tag{1}$$

e_1, e_2, and h_1, h_2 are the components of the vectors $\mathbf{e} = (\epsilon_o/\mu_o)^{1/4}\mathbf{E}$, and $\mathbf{h} = (\mu_o/\epsilon_o)^{1/4}\mathbf{H}$ in the rotating frame having the axis x_1 along the optical axis; ϵ_i and μ_i $(i=1,2)$ are the principal values of ϵ and μ, respectively; $\tilde{q} = qc/\omega$, where $q = 2\pi/p$ and p is the helix pitch. Notice that the propagation equation contains a constant system matrix H, an unique case in the literature of periodic media. The eigenwaves are $\tilde{\alpha}^{\pm}_{1,2}(x_3) = \alpha^{\pm}_{1,2} \exp(i\omega n^{\pm}_{1,2} x_3/c)$, where the time factor $\exp(-i\omega t)$ is omitted; $n_i^{\pm}$ $(i=1,2)$ are the eigenvalues of H, given by the dispersion relation

$$n^2_{1,2} = a_1 + \tilde{q}^2 \mp \sqrt{a_2\tilde{q}^2 + a_3^2}, \tag{2}$$

with $a_1 \equiv (\epsilon_1\mu_2 + \epsilon_2\mu_1)/2$, $a_2 \equiv 2a_1 + \epsilon_1\mu_1 + \epsilon_2\mu_2$, $a_3 \equiv (\epsilon_1\mu_2 - \epsilon_2\mu_1)/2$; and $\alpha_i^{\pm}$ are the corresponding eigenvectors, which are defined by the ratios of their components and will be normalized to unit energy density. Their polarization state is defined by the ratio

$$r_e \equiv e_2/e_1 = i\tilde{q}n(\mu_1 + \mu_2)/(\mu_2 n^2 + \mu_1\tilde{q}^2 - \epsilon_2\mu_1\mu_2), \tag{3}$$

where n is given by Eq. (2), and by the ratio $r_h \equiv h_2/h_1$, which is obtained by exchanging ϵ_i and μ_i in Eq. (3).

When ϵ_i and μ_i are real n^2 is real and the wave vectors $\omega n/c$ are real or purely imaginary. Only the modes $1^{\pm}$ show a band gap for ω within $\omega_1 = qc/\sqrt{\epsilon_1\mu_1}$ and $\omega_2 = qc/\sqrt{\epsilon_2\mu_2}$, where $n_1^{\pm}$ are purely imaginary and r_e, r_h are real, as shown by Eq. (3). Thus, the eigenmodes $\tilde{\alpha}_1^{\pm}$ are linearly polarized, with $\mathbf{e}^{\pm}$ and $\mathbf{h}^{\pm}$ parallel to the optic axis x_1 for $\omega = \omega_1$. By increasing ω from ω_1 to ω_2 (we assume here $\omega_1 < \omega_2$) $\mathbf{e}^+$, $\mathbf{h}^+$ and $\mathbf{e}^-$, $\mathbf{h}^-$ rotate by $\pi/2$ *in opposite senses*. For each mode $\mathbf{e}, \mathbf{h}$ remain parallel during the rotation only if $\epsilon_1/\mu_1 = \epsilon_2/\mu_2$. For different values of ϵ_i μ_i they make an angle $\psi = \cos^{-1}[(1 + r_e r_h)(1 + r_e^2)^{-1/2}(1 + r_h^2)^{-1/2}]$, which plays a main role for the properties of the defect mode. The dependence of ψ on ω and on the material parameters is shown in Fig. 1.

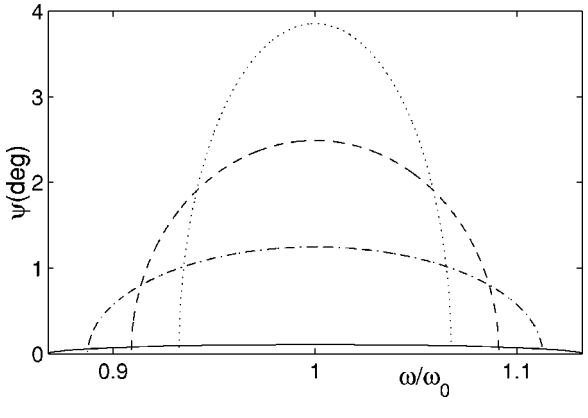

FIG. 1. ψ versus ω/ω_o, where ψ is the angle between the vectors $\mathbf{e}$ and $\mathbf{h}$ for the modes $1^{\pm}$, $\omega_o = (\omega_1 + \omega_2)/2$, $\epsilon_2 = 3$, $\mu_2 = 1$, $\epsilon_1/\epsilon_2 = 1.31$, $\mu_1/\mu_2 = 1, 1.1, 1.2$, and 1.3 (dotted, dashed, dash-dotted, and solid lines, respectively). The magnetic anisotropy plays here the role of a control parameter for the angle ψ.

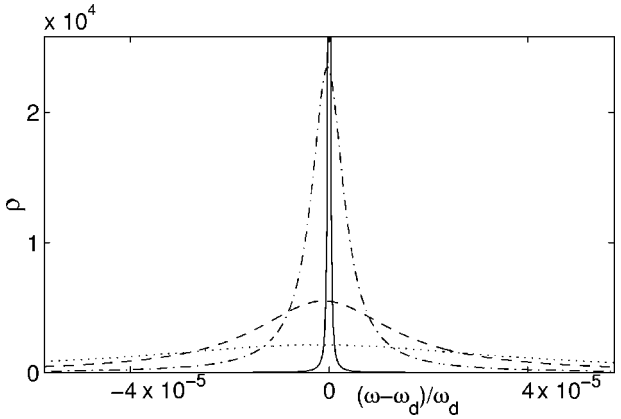

FIG. 2. ρ versus $(\omega-\omega_d)/\omega_d$, where ρ is the ratio between the square amplitudes of the localized and nonlocalized components and ω_d is the defect frequency. The twist angle is 45°, the values of ϵ_i, μ_i, and the symbols of the curves are the same as in Fig. 1. The solid curve is only partially within the figure since its maximum is equal to 1.18×10^5.

Within the gap the polarization of the eigenmodes $\alpha_2^{\pm}$ is nearly circular.

We consider now a lossless medium between the planes $x_3=-\ell$ and $x_3=\ell$ with a discontinuity plane at $x_3=0$, where the optical axes at the two sides of the plane make an angle 2ϕ (twist angle). For $x_3<0$ the electromagnetic field can be written as $f_\alpha(x_3)=a_1^+\tilde{\alpha}_1^+ + a_1^-\tilde{\alpha}_1^- + a_2^+\tilde{\alpha}_2^+ + a_2^-\tilde{\alpha}_2^-$. For $x_3>0$ it has a similar expression $f_\beta(x_3)$ with $a_i^{\pm}$ substituted by coefficients $b_i^{\pm}$ and $\tilde{\alpha}_i^{\pm}$ by functions $\tilde{\beta}_i^{\pm}$, obtained from $\tilde{\alpha}_i^{\pm}$ by applying a 2ϕ rotation to the vectors **e** and **h**. Within the gap of *unbounded structures*, namely, in the limit $\ell\to\infty$, the coefficients of the exponentially diverging eigenmodes must be zero ($a_1^+=b_1^-=0$). The coefficients a_1^- and b_1^+ define a *localized* component, which depends on x_3 as $\exp(-|x_3|\ell_d^{-1})$, where $\ell_d^{-1}=\omega|n_1|/c$, whereas the coefficients $a_2^{\pm}$ and $b_2^{\pm}$ define a *nonlocalized* component. The six nonzero coefficients must satisfy four continuity conditions, since $f_\alpha(0)=f_\beta(0)$. For any ω within the gap they admit solutions with $a_1^-=b_1^+=1$ and $|a_2^+|=|a_2^-|=|b_2^+|=|b_2^-|=m(\omega)$. The ratio $\rho(\omega)=1/2m^2$ between the square amplitudes of the localized and nonlocalized components has an enhanced maximum for a given frequency ω_d, as shown in Fig. 2. This solution defines therefore a quasilocalized defect mode with defect frequency ω_d.

The width of the function $\rho(\omega)$ depends strongly on the angle ψ plotted in Fig. 1. It is easy to show that when $\psi=0$ the defect frequency satisfies the relation

$$2\phi = \tan^{-1} r_e(\omega_d) + \tan^{-1} r_h(\omega_d), \tag{4}$$

and that $m(\omega_d)=0$, $\rho(\omega)=\delta(\omega-\omega_d)$. In fact for $\omega=\omega_1$ the vectors $\mathbf{e}_a, \mathbf{e}_b$ of the eigenwaves $1^{\pm}$ at the two sides of the defect plane make an angle 2ϕ, because they are parallel to the local optical axes. By increasing ω they rotate in opposite senses and become coincident at the bisector of the twist angle, namely, for a value ω_d such that $r_e(\omega_d)=\tan\phi$. For $\psi=0$, $r_h=r_e$ and the continuity conditions admit a solution with $m(\omega_d)=0$. For $\psi\neq0$, $m(\omega)$ is everywhere different from zero and such to make **e** and **h** parallel to the bisector of the twist angle.

The lifetime τ of the quasilocalized mode in actual samples is given by the ratio between the electromagnetic energy stored by the sample and the total power of the outgoing waves. It depends on the sample thickness 2ℓ and on the impedance mismatch at its boundaries. In the limit case of perfect matching the external and internal waves coincide. Thus, the defect mode represents the stationary internal field generated by two waves with identical amplitudes incident at both sides of the sample. It is easy to find $\tau(\ell)$ if we neglect the contribution of the nonlocalized component to the stored energy. Within the above approximations

$$\rho(\omega) \approx \rho(\omega_d)[1 + a^2(\omega-\omega_d)^2]^{-1}, \tag{5}$$

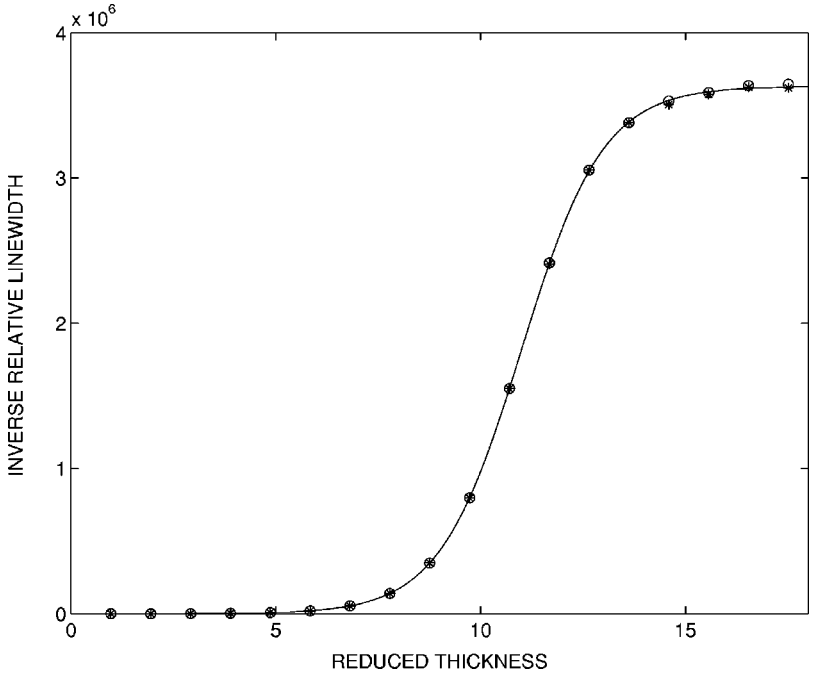

FIG. 3. Comparison between the inverse relative line widths $\omega_d/\Delta\omega$ of the transmittance curves versus $2\ell/\ell_d$ computed numerically (stars and circles for left and right circularly polarized waves, respectively), and the value derived from the quantity $\tau=(\Delta\omega)^{-1}$ given by Eq. (6) (solid line), in a sample with twist angle of $2\phi=90°$, $\epsilon_1=3.1$, $\epsilon_2=3$, $\mu_1=\mu_2=1$ within isotropic media with $\epsilon=3.05$.

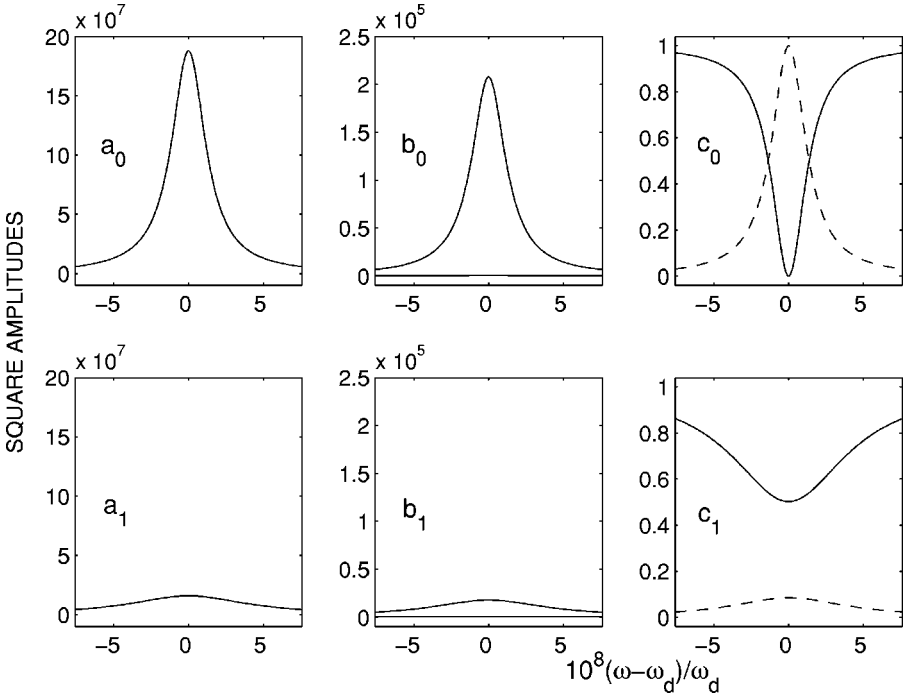

FIG. 4. Comparison between the scattering properties of a twist defect in lossless (upper curves) and lossy (lower curves) media. The figure gives the square moduli t_{ij} and r_{ij} of the elements of the scattering matrix of the defect plane, giving its transmission (solid lines) and reflection properties (dotted lines) versus $10^8(\omega-\omega_d)/\omega_d$ in a sample with twist angle $2\phi=\pi/50$, $\epsilon_1=3.6$ and $\mu_1=\mu_2=1$; the indices i, j refer to the incident and scattered waves; t_{11} and r_{11} are plotted in a_m; t_{21}, t_{12}, r_{21}, and r_{12} in b_m; t_{22} and r_{22} in c_m, where $m=0$ corresponds to $\epsilon_2=3$, and $m=1$ to $\epsilon_2=3+2\,i\,10^{-7}$. Note that t_{11} practically coincides with r_{11}, t_{12} with r_{12}, t_{21} with r_{21} ($t_{21}\ll t_{12}$), and that the small imaginary part decreases drastically the height of the peaks.

$$\tau(\ell) \approx \frac{\rho(\omega_d)\ell_d[1-\exp(-2\ell/\ell_d)]}{2v_m[1+\rho(\omega_d)\exp(-2\ell/\ell_d)]}, \tag{6}$$

where ω_d is given by Eq. (4); $\rho(\omega_d)=1/\sin^2(\psi/2)$; $a=\rho(\omega_d)\ell_d/(2v_m)\equiv\tau(\infty)$ and $v_m=2c/\sqrt{(\epsilon_1+\epsilon_2)/(\mu_1+\mu_2)}$. The internal field generated by a single external wave is the superposition of the quasilocalized defect mode and of nonlocalized modes, since Maxwell equations admit four independent solutions. It is quasilocalized but strongly asymmetric, in agreement with the simulations cited in Ref. 3. Its lifetime is still approximately given by Eq. (6), which for a small impedance mismatch at the sample boundaries can be used to compute the spectral width $\Delta\omega\equiv\tau^{-1}$ of the transmittance and reflectance curves for any practical purpose, as shown in Fig. 3.

Let us now discuss how the above properties change in the presence of absorption, by assuming that at least one of the material parameters ϵ_i, μ_i is complex (an exhaustive theory of lossy media is beyond the aim of this paper). Equations (1)–(3), which are still valid, show that the eigenvalues n_i of H and the components e_i, h_i of its eigenvectors become complex. Thus, also the eigenwaves $\tilde{\alpha}_2^+$ and $\tilde{\beta}_2^-$ diverge for $\ell\to\infty$ and must be discarded. The continuity conditions give four homogeneous equations in the four variables (a_i^-, b_i^+), which admit no solutions in general. The defect frequency ω_d corresponds to the ω-value which minimizes the determinant of the coefficients and is still approximately given by Eq. (4), whereas Eqs. (5) and (6) lose their validity even for very small values of the absorption coefficients, as a consequence of the changes induced by absorption in **e** and **h**, and of the critical role of the angle ψ between such vectors. In particular, the scattering properties of the defect plane change drastically, as shown in Fig. 4.

On the basis of the previous analysis it is possible to clearly explain the results already found numerically[3,5] and experimentally,[4,6] and to find optical properties of samples

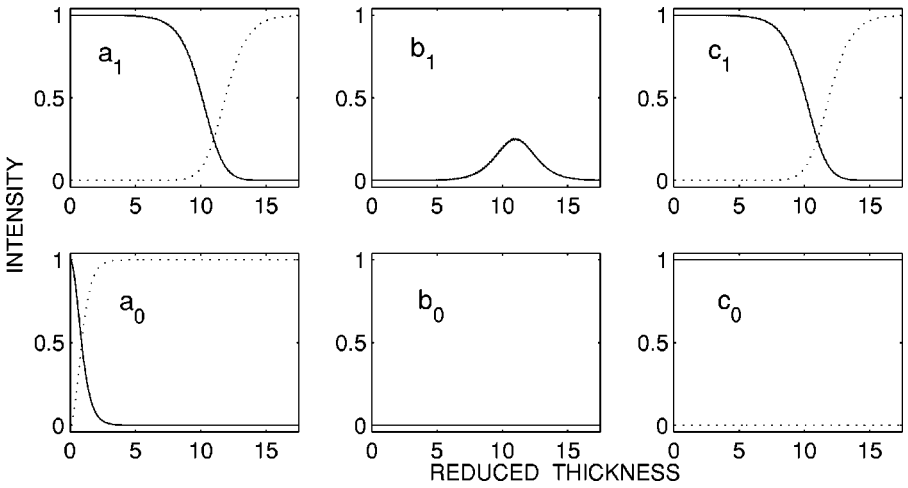

FIG. 5. Transmittance (solid lines) and reflectance (dotted lines) versus $2\ell/\ell_d$ for RC-RC (a_m), RC-LC and LC-RC (b_m), LC-LC (c_m) polarization of samples with (upper curves, $m=1$) and without (lower curves, $m=0$) the twist defect. The parameters are the same as in Fig. 3.

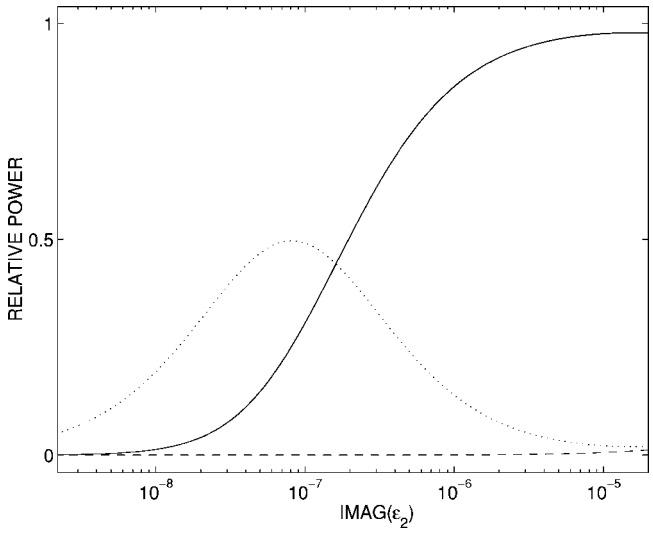

FIG. 6. LC-LC transmittance (solid line) and absorbance (dotted line) versus ϵ'' in a sample with $\ell = 6\ell_d$, twist angle of $\pi/50$, $\epsilon_1 = 3.6$, $\epsilon_2' = 3 + i\epsilon''$, $\mu_1 = \mu_2 = 1$. The dashed line gives the absorbance in a sample with the same material parameters but without the twist defect.

with twist defects, some of which are expected to have an acoustic analog.[8] Only a very few such properties are discussed here, by considering right-handed samples with small impedance mismatch at their boundaries without (Fig. 5) and with (Fig. 6) absorption. In these samples the eigenwaves 1 and 2 are excited by right and left circularly (RC and LC) polarized waves, respectively.

Figure 5 shows that the twist defect drastically changes the transmittance and reflectance curves of the sample. Obviously, in the limit of vanishing thickness ($\ell \to 0$) the incident wave is in any case totally transmitted. By increasing ℓ, the RC-RC transmittance curves decrease and the reflectance curves increase, as expected. The twist defect shifts by an order of magnitude the crossover length ℓ_c where the two curves intersect because it greatly enhances the amplitude of the eigenwave 1, as shown in Fig. 4 (a_0). It has more dramatic effects on the LC-LC curves [compare Figs. 5 (c_0) with 5 (c_1)]. For $\ell \gg \ell_c$ the sample reflects totally the LC waves, as suggested by the dotted curve of Fig. 4 (c_0). For $\ell \approx \ell_c$ the LC-LC curves intersect and mode-exchange peaks appear [Fig. 5 (b_1)], as a consequence of the scattering properties of the defect plane shown in Fig. 4 (b_0) and of the interference between the waves reflected at the defect plane and at the sample boundaries. The interesting effect found numerically by Kopp and Genack,[3] namely, the fact that the full curve of Fig. 5 (a_1) and the dotted curve of Fig. 5 (c_1) cross, receives here a clear explanation. An even more surprising effect of the twist defect is that the LC-LC curves of Fig. 5 (c_1) become practically coincident with the RC-RC curves of Fig. 5(a_1).

Figure 6 shows that in lossy media an increase of the absorption parameter ϵ'' does not decrease but hugely increases the transmittance (solid line), which goes from zero to nearly one in the ϵ''-interval where the reflection peak of Fig. 4 (c_0) disappears. An even more surprising effect concerns the total absorption within the sample (dotted line). In fact, in a large ϵ''-interval *an increase of the absorption parameter* ϵ'' *drastically decreases the absorbance*, which becomes practically the same as in a sample without the twist defect (dashed line). In this interval the peaks shown in Figs. 4(a)–4(c) practically disappear. This is an effect which overcomes the well-known effects of dissipation.

In conclusion, the theory developed here: (i) explains the scattering properties of lossless samples with a twist defect already found numerically and allows us to find other properties; (ii) shows that even a very small absorption destroys the optical effects due to the presence of the defect, giving rise to different and unexpected effects; and (iii) provides a solid basis for future research and applications since it evidences the existence of very critical parameters and defines frequency, lifetime, and spectral width of the defect mode by fully analytic and very simple equations; to our knowledge they are the simplest ones appearing in the literature of photonic band gap materials. For such reasons the interest of the developed theory goes beyond the helical structures considered here.

*On leave from Instituto de Física, Universidad Nacional Autonoma de Mexico, Apdo P. 20-364 01000, Mexico D. F.

[1] E. I. Kats, Zh. Eksp. Teor. Fiz. **59**, 1854 (1970) [Sov. Phys. JETP **32**, 1004 (1971)].

[2] J. J. Hodginsons *et al.*, Opt. Commun. **184**, 57 (2000).

[3] V. I. Kopp and A. Z. Genack, Phys. Rev. Lett. **89**, 033901 (2002); see also the Comment by C. Oldano, *ibid.* **91**, 259401 (2003), and the Reply of the authors.

[4] V. I. Kopp *et al.*, Proc. SPIE **4655**, 141 (2002).

[5] F. Wang and A. Lakhtakia, Opt. Commun. **215**, 79 (2003).

[6] J. Schmidtke, W. Stille, and H. Finkelmann, Phys. Rev. Lett. **90**, 083902 (2003).

[7] J. Schmidtke and W. Stille, Eur. Phys. J. E **12**, 553 (2003).

[8] C. Oldano, J. A. Reyes, and S. Ponti, Phys. Rev. E **67**, 056624 (2003).